

Middle Atmospheric Ozone Sounding by the ENVISAT/GOMOS Stellar Occultation Sensor

C. Retscher¹, G. Kirchengast¹, and A. Hauchecorne²

(1) Institute for Geophysics, Astrophysics, and Meteorology (IGAM), University of Graz, Austria

(2) Service d'Aéronomie du CNRS, Verrières-le-Buisson, France

christian.retscher@uni-graz.at

Abstract – We present results of an ozone retrieval algorithm developed to process data of the Global Ozone Monitoring by Occultation of Stars (GOMOS) instrument on board the environmental satellite ENVISAT. This instrument is, due to its high sensitivity, a promising tool to retrieve high accuracy profiles of several trace gases in the atmosphere from radiometric measurements. We concentrated on data between 250 nm and 340 nm and prepared our retrieval by following the Bayesian approach for an optimal combination of *a priori* data and new measurements. Using a fast converging iterative optimal estimation algorithm intrinsically including proper forward modeling we found good performance in ozone profiling. Best accuracies were found in altitudes between 20 km and 50 km. Once ENVISAT provides real data the whole processing chain is expected to yield better performance in the profiling of ozone than algorithms used so far.

I. INTRODUCTION

The mapping of high accuracy ozone profiles is crucial for a deeper understanding of changes in the composition of the atmosphere and has a substantial impact on long-term climate prediction. Stratospheric heating due to the absorption of UV radiation and the importance of ozone as a greenhouse gas are strongly connected to the effects of its continuing depletion. As the primary absorber of solar radiation in the middle UV, ozone plays as well a central role for the biosphere on the Earth surface. Detailed global measurements of the vertical and the horizontal distribution of ozone are therefore necessary to conceive physical and photochemical processes.

The European Environmental Satellite ENVISAT, recently (on 1 Mar 2002) launched for a > 5 year mission, is ESA's most comprehensive and prestigious venture for probing land, ocean, ice, and the atmosphere.

The Global Ozone Monitoring by Occultation of Stars (GOMOS) sensor on-board ENVISAT is a self-calibrating instrument intended to provide data on trace gases such as ozone, NO₂, NO₃, BrO, OClO, as well as O₂ and water vapor. It is the first instrument using the stellar occultation technique for ozone profiling. A special instrument design makes it possible to measure reference atmospheric profiles in dark and bright limb obtaining very good global

coverage with about 300 high-quality profiles per day and a height resolution of about 1.5 km. GOMOS records the transmission of radiation passing the atmosphere along a path from the star to the instrument.

The so-called Spectrometer A measures ozone, NO₂, NO₃, BrO, and OClO within a wavelength range from 250 nm to 675 nm and has a resolution of 1.2 nm. The Spectrometers B1 and B2 are sensitive within 756–773 nm and 926 nm–952 nm, respectively, with 0.2 nm resolution, and were designed to measure O₂ and water vapor.

Here we present results of our preliminary ozone retrieval algorithm based on cross-section data of the GOMOS standard cross-section database, standard climatological atmospheric profiles for the trace gases, and CIRA model profiles for background temperature and pressure. The algorithm is designed in such a way as to guarantee a seamless interface to GOMOS level 1b data [ACRI S.A. et al., 1998; Paulsen, 2000].

II. GOMOS ALGORITHMS

The formulation of an appropriate signal propagation geometry is of major importance in order to develop a realistic forward model procedure. We use a realistic yet fast raytracing algorithm, which solves the refractive raypath problem with the star and the satellite position as boundary conditions.

The atmospheric transmission is given by Beer-Bouguer-Lambert's law, at each frequency of interest ν , as

$$T_\nu = \frac{I_\nu(s)}{I_\nu(0)} = \exp \left[- \int_0^s \sum_i n_i(s') \sigma_{i\nu}(s') ds' \right]. \quad (1)$$

The transmission T_ν is a ratio of the radiation intensity measured in the atmosphere, $I_\nu(s)$, relative to the one, $I_\nu(0)$, measured above (height ~ 100 km) the atmosphere. Due to the motion of the spacecraft, the line of sight dives deeper and deeper into the atmosphere, while the signal gets increasingly attenuated. The integral is carried out along a refracted ray path s . The number densities n_i and the cross sections $\sigma_{i\nu}$ are associated with the species ozone and NO₂

in our context. Given the magnitude of bulk air density in the lower stratosphere, we include a term for Rayleigh scattering as well. In this baseline work a term for the aerosol extinction was neglected, nevertheless, we plan to introduce it in future refinements. Since stars can be assumed to provide a point signal, no further integration over a finite field of view has to be done (as may, e.g., be required for solar occultation).

Having a forward model established, we now have to find an inverse connection between measurements (transmission data) and targeted state (ozone profile) of the atmosphere. Discrete inverse theory provides such a framework. The forward model can be seen as an algebraic mapping of the state space into the measurement space. We introduce an operator \mathbf{K} , which here will be the Jacobian matrix with the dimension $m \times n$ for m measurements and n elements of the state vector. By taking the measurement error $\boldsymbol{\varepsilon}$ into consideration the forward modeling reads

$$\mathbf{y} = \mathbf{K}(\mathbf{x}) + \boldsymbol{\varepsilon}. \quad (2)$$

The sensitivity of measured transmissions \mathbf{y} to the state \mathbf{x} , the ozone density profile, can be interpreted as “weighting functions” and seen represented by the rows of \mathbf{K} .

Because of the generally non-linear Eq. (2), it is obvious that a straightforward solution for \mathbf{x} by direct inversion is not feasible. The direct inverse mapping, if $\mathbf{K}(\mathbf{x}) = \mathbf{K} \cdot \mathbf{x}$ (i.e., linearity applies), would be

$$\mathbf{x}_r = \mathbf{K}^{-g} \mathbf{y}, \quad (3)$$

where \mathbf{K}^{-g} denotes a general inverse matrix and \mathbf{x}_r is the retrieved state. As the problem of interest here is somewhat ill-conditioned at high altitudes (it may also be over-determined if we use more measurements than unknown states; $m > n$), we cannot directly employ Eq. (3) but rather constrain the solution by incorporating sensible *a priori* information. The Bayesian approach is the method of choice to solve such inverse problems perturbed by noise, where we have rough but reliable prior knowledge of the behavior of a state of interest. We can enhance this prior knowledge in a consistent way by incorporating new measurements with the Bayesian approach.

With the assumption of Gaussian probability distributions and a linearized forward model, we make use of a fast converging iterative optimal estimation algorithm [Rodgers, 2000],

$$\mathbf{x}_{i+1} = \mathbf{x}_{ap} + \mathbf{S}_i \mathbf{K}_i^T \mathbf{S}_\varepsilon^{-1} \left[(\mathbf{y} - \mathbf{y}_i) + \mathbf{K}_i (\mathbf{x}_i - \mathbf{x}_{ap}) \right], \quad (4)$$

with the associated optimal error covariance,

$$\mathbf{S}_i = \left(\mathbf{K}_i^T \mathbf{S}_\varepsilon^{-1} \mathbf{K}_i + \mathbf{S}_{ap}^{-1} \right)^{-1}. \quad (5)$$

In Eq. (4), \mathbf{x}_i is the retrieved and \mathbf{x}_{ap} the *a priori* profile. Key ingredients of Eq. (5) are the *a priori* covariance

matrix \mathbf{S}_{ap} and the measurement error covariance matrix \mathbf{S}_ε . The Jacobian (also called weighting) matrix \mathbf{K}_i represents the mapping involved. Index i is the iteration index; the iteration was started by using $\mathbf{x}_0 = \mathbf{x}_{ap}$.

For the elements of \mathbf{S}_{ap} we considered typical errors expected in prior ozone and NO_2 profiles and assumed uncertainties of 20% and 40%, respectively, for the diagonal elements. Off-diagonal elements were modeled by an exponential drop-off correlation of the form

$$S_{ij} = \sigma_i \sigma_j e^{-|z_i - z_j|/L}, \quad (6)$$

where z_i and z_j denotes the height levels between which the covariance is expressed, and where L denotes a correlation length set to 6 km in order to reflect the fact that prior profiles are usually fairly smooth at scales smaller than an atmospheric scale height. The standard deviation at a specific height level, σ_i , corresponds to $\sigma_i = (\mathbf{S}_{ap})_{ii}^{1/2}$.

\mathbf{S}_ε was designed by adopting a 1% standard error at unity transmission and increasing errors with decreasing transmission according to the square-root law, i.e., $(\mathbf{S}_\varepsilon)_{jj} = 0.01/(y_j^{1/2})$. Off-diagonal elements were assumed zero (i.e., no interchannel correlation). These error assumptions roughly reflect the measurement error specifications of the GOMOS sensor.

The raytracer-simulated actual transmission measurements, $\mathbf{y} = \mathbf{K}(\mathbf{x})$, where superimposed by stochastic error realizations $\boldsymbol{\varepsilon}$ (cf. Eq. 2) consistent with the \mathbf{S}_ε matrix. This was done with the same “error pattern method” as outlined below for \mathbf{S}_{ap} . The measurement vector estimate at any iteration step i , $\mathbf{y}_i = \mathbf{K}(\mathbf{x}_i)$, is used without further modification, however.

The *a priori* profiles \mathbf{x}_{ap} were derived by superimposing on the “true” state \mathbf{x} error realizations consistent with the *a priori* error covariance matrix \mathbf{S}_{ap} . For this purpose the “error pattern method” was used [cf., e.g., Rodgers, 2000; Weisz, 2001], which exploits the fact that one can decompose \mathbf{S}_{ap} into so-called error patterns $\mathbf{e}_i = \sqrt{\lambda_i} \mathbf{I}_i$ obeying $\mathbf{S}_{ap} = \sum_i \mathbf{e}_i \mathbf{e}_i^T$. The error patterns \mathbf{e}_i are the eigenvectors of \mathbf{S}_{ap} , \mathbf{I}_i , weighted by the square-root of the eigenvalues λ_i . In order to construct \mathbf{x}_{ap} statistically consistent with \mathbf{S}_{ap} , one adds an error vector $\Delta \mathbf{x} = \sum_i a_i \mathbf{e}_i$ to the “true” state \mathbf{x} , where the scalar coefficients a_i are normal random deviates drawn from a normalized (zero mean and unit variance) Gaussian distribution.

In general, an error analysis and characterization of atmospheric profile retrievals is an important task for every sensor. Bayesian optimal estimation provides a very suitable framework for this purpose as, for example, demonstrated by Rieder and Kirchengast (2001) for radio occultation data.

III. ANALYSIS FOR OZONE PROFILES

We performed tests of our preliminary algorithm based on a realistic occultation event. The geometry of the event, displayed in Figure 1, was provided by ESOPS (End-to-end Signal Occultation Performance Simulator), a comprehensive occultation simulation tool currently under development as enhancement of EGOPS (End to end GNSS Occultation Performance Simulator) [Kirchengast, 1998; Kirchengast et al., 2001]. The realistic star and ENVISAT locations during the event were used as boundary conditions for the forward modeling.

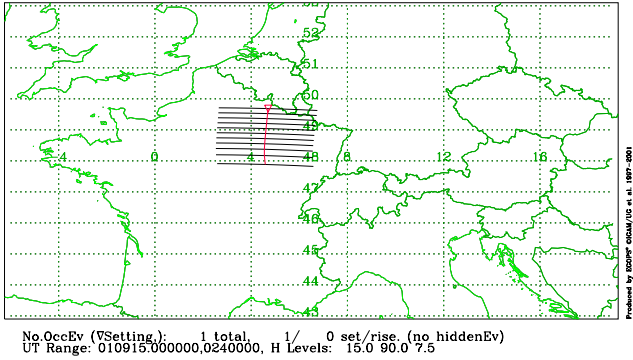


Figure 1. Test occultation event with 7.5 km spacing between rays from 90 km to 15 km along the tangent point trajectory in nadir view over north-eastern France and southern Belgium. The bundle of parallel lines shows the raypaths for ± 150 km about the tangent point, roughly reflecting the horizontal resolution of the occultation data.

In this baseline study we adopted spherically symmetric atmospheric profiles in the forward modeling, though our fast ray tracing algorithm calculates the raypath by taking also horizontal variations of refractivity and of vertical refractivity gradients into account (this capability will be useful in future more elaborated application). We simulated the scanning of the atmosphere with a sampling rate of 2 Hz, from altitudes of 90 km to 15 km, and retrieved ozone profiles at a retrieval grid with 1 km spacing. This is a slightly overdetermined mode (as 2 Hz data relate to about 1.5 km spacing), which is no problem for the algorithm employed, however. Simulated transmission profiles, after carrying through the forward modeling according to Eq. (1), are displayed in Figure 2.

In contrast to the GOMOS operational retrieval, where the forward model uses all many hundred channels of Spectrometer A, we restrict ourselves to only ten channels (here 260, 275, 290, 300, 310, 320, 325, 330, 335, and 340 nm) as Figure 2 illustrates. We therefore gain vastly in computational efficiency while retaining quality of the ozone profiles on which we focus. The current operational algorithm simultaneously retrieves all accessible species (see section I) and involves no stabilization at high altitudes by prior information. The channel selection will be further optimized in the future, especially within 320 and 340 nm.

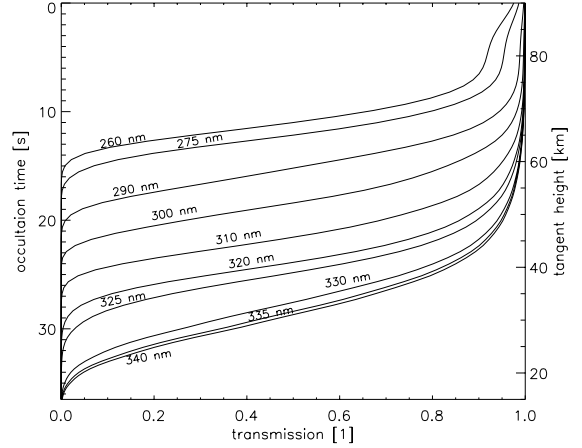


Figure 2. Simulated transmission profiles based on including O_3 , NO_2 , and NO_3 absorption as well as Rayleigh scattering for the 10 channels used for in this baseline study.

As in the selected wavelength range ozone absorption reaches its maximum, while ozone cross sections show only slight temperature dependencies; this range provides the most favorable GOMOS channels for ozone retrieval. In order to ensure high reliability of retrieved ozone profiles also at heights dominated by the spectral region > 320 nm, we also included NO_2 into the state vector and performed a simultaneous NO_2 retrieval.

Using the transmissions shown in Figure 2, perturbed by noise as discussed above, the retrieval was carried out according to Eqs. (4) and (5). A one-step retrieval was done only (to obtain x_1 and S_1) as convergence was essentially achieved already with this step. The detailed convergence properties in case of our problem will be investigated in the near future. Figures 3 and 4 illustrate the retrieval results obtained for a representative test case. Errors of $< 2\%$ in ozone density are seen at all heights, which is encouraging for further advancements of the algorithm.

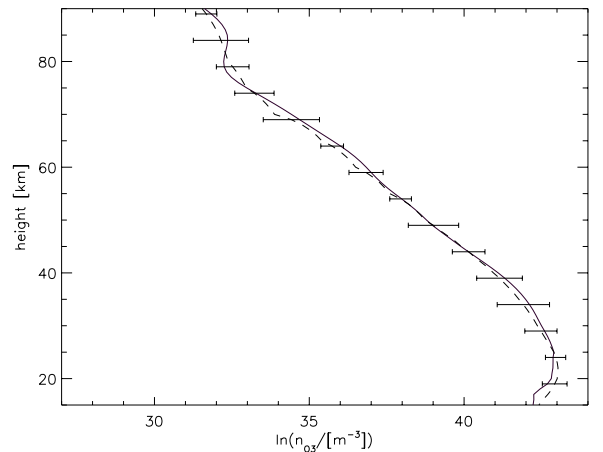


Figure 3. Example of retrieved ozone number density profile (solid line) with the “true” profile (dashed line) shown for reference. Error bars indicate the standard deviation $(\pm(S_1)_i)^{1/2}$ estimate of Eq. (5).

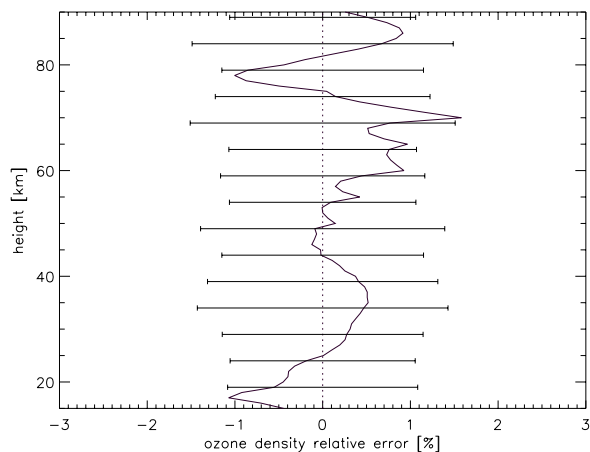


Figure 4. Relative errors of the retrieved ozone density profile shown in the previous figure (difference retrieved-minus-“true”). Error bars again indicate the standard deviation estimate of Eq. (5).

IV. SUMMARY AND CONCLUSION

We developed an optimal estimation algorithm for retrieval of atmospheric profiles from ENVISAT/GOMOS-measured transmission data. In this study ozone profiles were retrieved, which is the primary focus of the algorithm, though the whole processing chain is capable of retrieving other trace gases simultaneously. Furthermore, complementary exploitation of atmospheric bending angles derived from GOMOS star tracker data (“SATU/SFA data”) was neglected in this study but will be introduced as a future enhancement. These data will allow to simultaneously retrieve temperature profiles in the lower stratosphere as well as atmospheric refractivity, which can be used to improve the background climatology required by the raytracing. These advancements will, in turn, further improve the ozone retrieval.

In conclusion, the approach adopted for an efficient and effective retrieval of ozone profiles has yielded encouraging preliminary results so far, with ozone profile accuracy better than 2% throughout the stratosphere and mesosphere. We are thus confident to be able to start applying the algorithm to real GOMOS data by summer 2002.

ACKNOWLEDGMENTS

The authors gratefully acknowledge discussions with and support by U. Foelsche, M. Schwärz, C. Rehl, and J. Ramsauer (IGAM, Univ. of Graz, Austria). Special thanks go to G. Barrot (ACRI S.A., Sophia Antipolis, France) for providing simulated GOMOS data. The European Space Agency is thanked for operating the ENVISAT satellite and for its related Announcement of Opportunity for free access to ENVISAT data, which will be vital in subsequent work. C.R. received financial support for the work from ENVISAT Project AO-620/Part-I funded by the Austrian

Ministry for Traffic, Innovation, and Technology and carried out under contract with the Austrian Space Agency.

REFERENCES

- ACRI S.A., Finnish Meteorol. Institute, Service d’Aéronomie du CNRS, Institut d’Aéronomie Spatiale de Bruxelles, “GOMOS High Level Algorithms Definition Document,” <http://envisat.esa.int/support-docs/>, 1998.
- G. Kirchengast, “End-to-end GNSS Occultation Performance Simulator overview and exemplary applications,” Wissenschaftl. Ber. No. 2/1998, Inst. for Meteorol. and Geophys., Univ. of Graz, Austria, 1998.
- G. Kirchengast, J. Fritzer, and J. Ramsauer, “End-to-end GNSS Occultation Performance Simulator Version 4 (EGOPS4) Software User Manual (Overview and Reference Manual),” Tech. Rep. for ESA/ESTEC-5/2001, Inst. for Geophys., Astrophys., and Meteorol., Univ. of Graz, Austria, 2001.
- T. Paulsen, “GOMOS Level 1b/2 Algorithm Description document for Envisat pre-release,” ESA Doc. PO-TN-ESA-GM-1019, ESA/ESTEC, Noordwijk, Netherlands, 2000.
- M. J. Rieder, G. Kirchengast, “Error analysis and characterization of atmospheric profiles retrieved from GNSS occultation data,” *J. Geophys. Res.*, 106, pp. 31755-31770, 2001.
- C. D. Rodgers, “Inverse Methods for Atmospheric Sounding: Theory and Practice,” 256pp., World Sci. Publ., Singapore, 2000.
- E. Weisz, “Temperature Profiling by the Infrared Atmospheric Sounding Interferometer (IASI): Advanced Retrieval Algorithm and Performance Analysis,” IGAM Wiss. Ber. No. 11, Inst. for Geophys., Astrophys., and Meteorol., Univ. of Graz, Austria, 2001.